



ORIGINAL ARTICLE

Excellent protection of mild steel in sodium chloride solution for a substantial period of time using a hybrid nanocoating of poly vinyl alcohol and Titania



P.K. Jaseela ^a, Mathew Kuruvilla ^b, Linda Williams ^a, Chinju Jacob ^b,
K.O. Shamsheera ^a, Abraham Joseph ^{a,*}

^a Department of Chemistry, University of Calicut, Calicut University P O, India

^b Department of Chemistry, St Thomas College, Ranni, Pathanathitta, India

Received 29 April 2020; accepted 2 July 2020

Available online 9 July 2020

KEYWORDS

Nanocomposite;
Hybrid material;
TiO₂;
PVA;
Corrosion inhibition

Abstract The production of eco-friendly hybrid sol–gel coatings for long term protection of metallic substrates from aggressive environments was one of the emerging areas, competing with conventional chromate and phosphate coatings. Herein, a nanocomposite has been synthesized from TiO₂ and PVA through a novel sol-gel route and the structure and morphology of the same was characterized using X-ray diffraction, FTIR, UV–Vis spectroscopy, FESEM with EDAX, and AFM studies. The flower-like structured composite offers excellent corrosion protection properties in NaCl solution of sea water salinity. Impedance and polarization studies were carried out to monitor the anticorrosion performance of the materials coating. This coating on mild steel offers 98% inhibition efficiency in NaCl. The influence of loading PVA on TiO₂ and its effect on corrosion efficiency have also been investigated. It is found that an optimum weight of 20 wt% PVA is required in the composite for beneficial corrosion resistance. 92% inhibition efficiency is registered by the coated MS in NaCl solution after 40 days of exposure and is quite encouraging compared to many of the recent reports. The Ti–O–Ti, and Fe–Ti–O linkage along with compactness and adherence of the material together contribute to better blocking of steel corrosion.

© 2020 The Author(s). Published by Elsevier B.V. on behalf of King Saud University. This is an open access article under the CC BY-NC-ND license (<http://creativecommons.org/licenses/by-nc-nd/4.0/>).

* Corresponding author.

E-mail address: abrahamjoseph@uoc.ac.in (A. Joseph).

Peer review under responsibility of King Saud University.



1. Introduction

The design and fabrication of flexible nontoxic hybrid materials in simple and viable methods are needed to meet the demands of industry for various purposes including the protection of metals/materials from aggressive environments. Mild steel is a common material used in industries due to low cost,

high tensile strength and availability. But its corrosion prone nature is a fundamental concern of industrialists and scientists which needs to be addressed using new materials and methods. Many disasters have reported from industrial sectors due to metallic corrosion through the interaction of materials and medium/electrolyte. The medium encountered in corrosion are usually electrolyte containing dissolved ionic species (Ramya et al., 2015; Anupama et al., 2015). The presence of chloride ions promotes rapid attack of metallic substrate and also localized attack depending on the concentration of electrolytic solutions/medium of corrosion. The pH of 3.5 wt% NaCl is normally near 5.8 at room temperature, which is more or less close to the salinity of sea water (Vignesh et al., 2017). For many decades corrosion prone metals were managed by using hexavalent chromate species, an eco-toxic material which is being replaced widely with more environmentally benign materials (Tsapakos et al., 1983; Liu et al., 2005; Chou et al., 2001). TiO₂ is widely accepted as an ideal candidate in the field of energy and environmental crisis. Its self-assembled 2D nanomaterials has been attracted scientists on account of the capability of achieving excellent properties upon modification as functional materials such as pollutant degradation, catalysis, water-purifications, biomedical materials, solar cells and protective materials such as coated layers on metals (Geng et al., 2020; Zhao et al., 2019; Ge et al., 2020; Wang et al., 2020; He et al., 2020; Zhang et al., 2017; Zhang et al., 2018). The use of sol-gel based Titania coatings is a very simple and most promising method (Luo et al., 2012; Sinapi et al., 2002) to protect different metals/materials in aggressive environments. The issue with simple TiO₂ coating on metals is the development of surface defects/cracks on prolonged exposure which adversely affect the efficiency of protection (Palomino et al., 2006). The development of a corrosion resistant hybrid material with both organic and inorganic moiety is an alternative way in which the organic part offers improvement in the adhesion characteristics of the coating while inorganic part enhances the hardness and the scratch resistance of the coating (Lakshmi et al., 2013). The sol-gel process allows the introduction of organic groups including polymers into the TiO₂ matrix easily and thus the method forms a promising strategy of developing a super protective coating with increased physical properties (Cohen, 1995; Van Ooij and Child, 1998; Zhu and van Ooij, 2003; Ning et al., 2012; Van Ooij et al., 2000; Donley et al., 2003; Zheludkevich et al., 2007; Wang and Bierwagen, 2009). M. Catauro et al. synthesized OIH materials by sol-gel method using TiO₂ for the inorganic matrix and poly(ϵ -caprolactone) as organic component. The material produced was used to improve the performance of Ti6Al4V implants (Catauro et al., 2017). Recently Hongjun Kan et al. was fabricated a novel nanostructured TiO₂ mesh membrane by a simple electrochemical anodization and heating process which showed anticorrosive ability (Kang et al., 2018). Xiaokun Cui et al. investigated the anticorrosion ability of the PDMS/TiO₂ composite coating on the AA 2024 (one of the aluminium alloy). The long term immersion experiments of coating were performed and the results demonstrated that the coating still had a protective effect on aluminum after 40 days of immersion (Cui et al., 2018). Balaji et al. have been made attempts to form smart/intelligent, corrosion resistant nanocomposite coatings through sol-gel process by self-assembly method. Chitosan-doped-hybrid/TiO₂ nanocomposite based sol-gel coating for the corrosion resistance of alu-

minum metal in 3.5% NaCl medium coating exhibited better protection from corrosion (Balaji and Sethuraman, 2017). Most of the data available in the literature suggest that OIH sol-gel materials have an enormous potential in the field of anticorrosion coatings. Recently many studies have focussed on eco-friendly TiO₂ based organic/inorganic nanocomposite films (Zheludkevich et al., 2007). Researchers applied various methods to improve the barrier properties and corrosion protection efficiency TiO₂ using inorganic-organic hybrid materials, however, these methods are cumbersome and economically non-viable. Utilizing the epoxy resin modified coating of Titania and PVA hybrid through in situ poly-condensation can obviously improve the corrosion protection properties of the material through better adhesion and high chemical and electrical resistances. There are a few experiments available in literature which deal with the anticorrosion protection properties of PVA with TiO₂ on the steel surface (Ramezanzadeh et al., 2015; Jaseela and Joseph, 2018). In this paper we focus on (1) the preparation of multifunctional hybrid TiO₂-PVA nanocomposite with very good anticorrosion properties (2) an in-expensive green modifier PVA is used for the development of corrosion resistant flower like nanocomposite coatings (3) characterization XRD, absorption spectra, FTIR, FESEM with EDAX, and AFM (4) evaluation and investigation of anticorrosion performance of hybrid coating on mild steel in NaCl solution.

2. Experimental part

2.1. Materials and methods

The reagents titanium ethoxide and poly vinyl alcohol are from Spectrochem Pvt. Ltd India and triethanolamine and sodium chloride Merck (India) Ltd. The pre and post treatment of mild steel specimens were done as per the ASTM recommendation.

2.2. Coating strategy

TiO₂-PVA sol was synthesized by the hydrolysis ethanolic solution of titanium ethoxide and triethanolamine. Ethanolic solution (50 mL) of titanium tetra ethoxide (6 mL) was mixed with triethanolamine (6 mL) and stirred using a magnetic stirrer for 15 min. 8 mL of distilled water was then added to this mixture dropwise and stirred for about 3 h at room temperature. A homogeneous TiO₂ sol was obtained on keeping the reaction mixture under stirrer for 2.5 h. A solution of PVA (0.2 g) dissolved in 25 mL water maintained at 70 °C was then added drop wise into TiO₂ sol with vigorous stirring for 3 h to obtain TiO₂-PVA nanocomposite. TiO₂-PVA sol with different weight percentage (10–30 wt%) of PVA was then prepared by similar method. The coatings modified with PVA at 10, 20, 30 wt% were named as TPVA₁, TPVA and TPVA₂ respectively. The surface preparation of mild steel coupons of composition (atom %): Fe(98.75%), C(0.2%), Mn (1%), S (0.02%), and P(0.03%) was carried out as per ASTM specifications. The dried metal coupon was then dip-coated by using a dip coater with a withdrawal speed of 10 mm/min. After air-drying, the coupons were dried in an oven at 130 °C for 1 h (gel densification step) and finally heat-treated in a muffle from 28 °C to 200 °C (5 °C/min) for 2 h.

2.3. Material characterization

The functional groups present on the coated metal surface was studied by using the scraped TPVA coating from the mild steel surface and made pellet with KBr and analysed using FTIR 4100 spectrometer (JASCO, Japan) in the range 400–4000 cm^{-1} . The UV-visible spectra of samples were recorded in 550 UV-Vis spectrophotometer (JASCO, Japan) in the range of 200–800 nm. The morphology and elemental composition of coated and bare mild steel were studied by FESEM and EDAX (FESEM, Zeiss, Germany). AFM studies of the samples were carried out by using APER-A-100 SPM (Germany) in contact mode. X-ray diffraction pattern was recorded using MINIFLEX-600 diffractometer (RIGAKU, Japan) with $\text{Cu K}\alpha$ ($\lambda = 1.5406 \text{ \AA}$) scanned in the range at 2θ 10° to 90° .

2.4. Corrosion tests

Corrosion protection properties of PVA loaded TiO_2 coating on mild steel were evaluated using impedance (EIS) and polarization (PDS) methods by exposing the metal coupon in 3.5 wt% NaCl solution using Gill AC potentiostat (model number 1475). A cell setup with three electrodes was used

for electrochemical studies, in which a platinum foil as a counter electrode, SCE as the reference electrode and the mild steel coupon as working electrode. Nyquist and Tafel data were recorded for both non-coated and coated metal specimens. Alternating Current impedance measurements were carried out at E_{corr} in the range from 0.1 Hz to 10 kHz with amplitude of 10 mV. The protection efficiency was calculated using charge transfer resistance using Eq. (1),

$$\text{IE}\% = \frac{R_{\text{Ct}}^* - R_{\text{Ct}}}{R_{\text{Ct}}^*} \times 100 \quad (1)$$

where R_{Ct}^* and R_{Ct} represents the charge transfer resistance for the coated and bare mild steel coupons.

The polarization behaviour of the material was studied at a scan rate of 60 mVs^{-1} and a scan range of -250 mV to $+250 \text{ mV}$ and protection efficiency was calculated using corrosion current density using Eq. (2)

$$\text{IE}\% = \frac{I_{\text{Corr}}^* - I_{\text{Corr}}}{I_{\text{Corr}}^*} \times 100 \quad (2)$$

where I_{Corr} and I_{Corr}^* represents the corrosion current density of the coated and bare mild steel coupons.

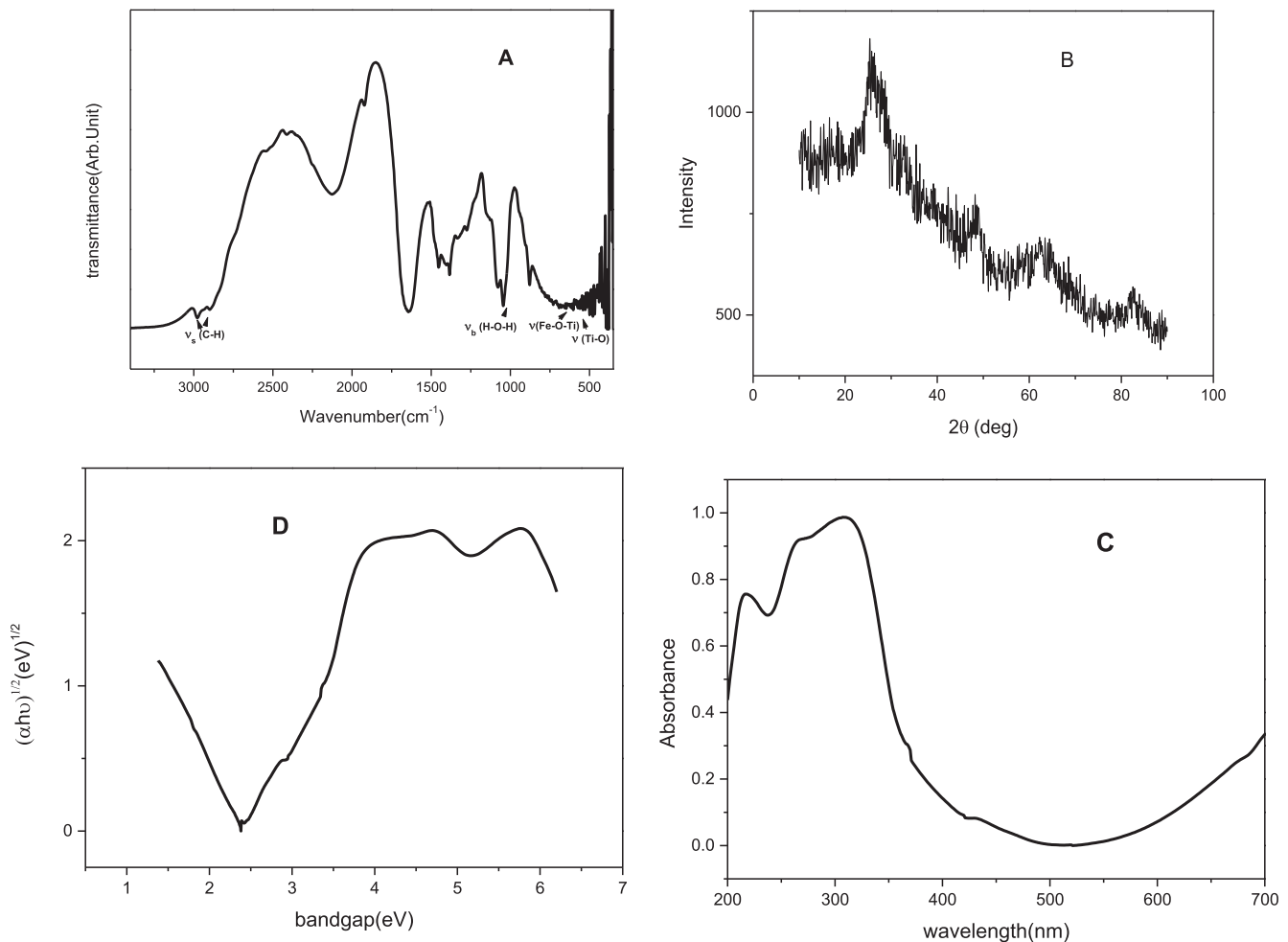


Fig. 1 (A) FTIR spectra (B) XRD (C) UV spectra (D) Tauc plot of TPVA composite coating on mild steel.

3. Results and discussion

3.1. Fourier transform infrared spectroscopy

The FTIR spectra of TPVA coating is shown in Fig. 1 A. Typically the Ti-O, Ti-O-Ti stretching and bending modes was in the range of 500–900 cm^{-1} which was slightly shifted to 400–700 cm^{-1} due to the introduction of PVA in the TiO_2 , confirmed the cross-linked structure of the hybrid nanocomposite. The band at 570 cm^{-1} could be assigned to the stretching mode of Fe-O-Ti bond (Kim et al., 2013). The presence of this bond further confirms the good adhesion of this sol-gel on metal surface through Fe-O-Ti bond. The band at 1079 cm^{-1} was

assigned for Ti-O-C stretching mode. The peak registered at 1,474 cm^{-1} was assigned to be the C-H bending vibration. The symmetric and anti-symmetric C-H stretching of methylene groups are registered at 2860 cm^{-1} 2931 cm^{-1} respectively (Vignesh et al., 2017; Karthik and Sethuraman, 2015; Das et al., 2008). The IR results clearly indicates the presence of a substantial amount of organic groups on the metal surface.

3.2. X-ray diffraction (XRD) studies

The X-ray diffraction patterns of TPVA coating is shown in Fig. 1B and this XRD pattern confirming that the amorphous TiO_2 particles present in the coating on mild steel are

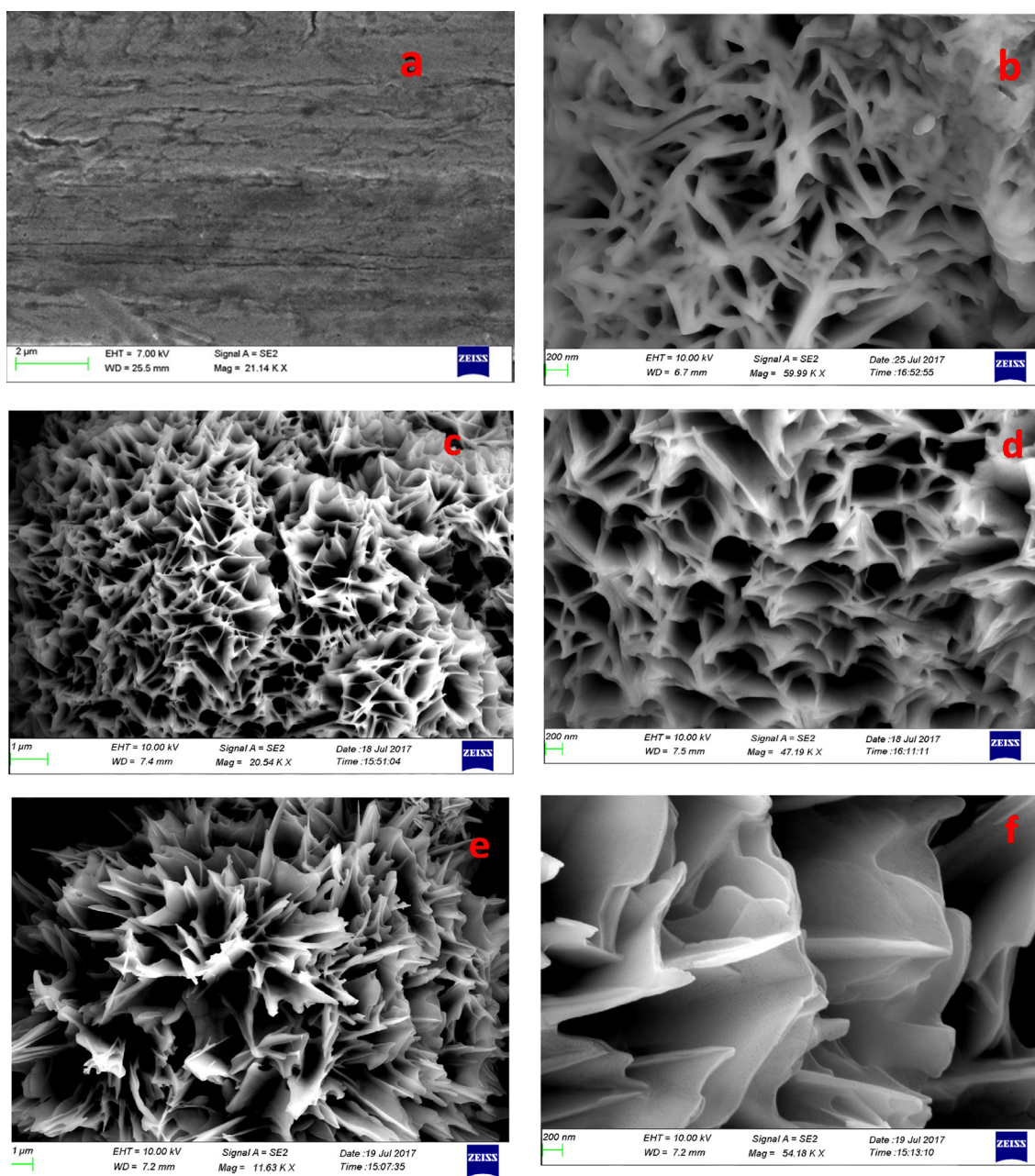


Fig. 2 FESEM image of (a) bare mild steel (b) TPVA₁ (c) and (d) TPVA₂ (e) and (f) TPVA coated on mild steel at different magnification.

nanosized (Zhang and Banfield, 2002). The major peaks obtained in the range 2θ equal to 25.35° , 48.63° , 62.58° from the planes (101), (200), and (213) respectively. The results are in accordance with the data base (JCPDS No 75–1537) showing the presence of complete anatase phase of titania in the coating on mild steel.

3.3. Absorbance spectra

The reflectance spectra (DRS) and Tauc plot of the material are shown in Fig. 1C and D. The peak in the region of 200–400 nm, corresponds the strong absorption in that region, is the characteristic peak of TiO_2 which confirms the presence of TiO_2 in the coating. The band gap energy calculated from Tauc plot is 2.1 eV. The lower band gap energy of the material would be a clear indication of its good inhibition efficiency by lowering the energy required to remove the most loosely bound electron from the HOMO (Anupama et al., 2016).

3.4. FESEM/EDAX analysis

Fig. 2 depict the field emission SEM image of bare and coated mild steel. Generally, pure TiO_2 coating results coating with cracks and enable localized attack of the material on prolonged use and PVA loading minimizes this tendency of the coating. The TiO_2 -PVA nanocomposite exhibit flower-like distribution on the metal surface and get uniformly coated on metal surface without any cracks. This stable coating will not allow the passage of solvents or other ions responsible for the material deterioration. It can be seen from Fig. 3 that after 40 days of exposure of the coated material in NaCl, the metal surface has uniform coating and good barrier properties. The EDAX spectrum given in Fig. 3 C which obtained from the surface scrap after 40 days of immersion in NaCl solution shows peaks corresponding to TiO_2 and C and N which could be due to the presence of organic part in the coating.

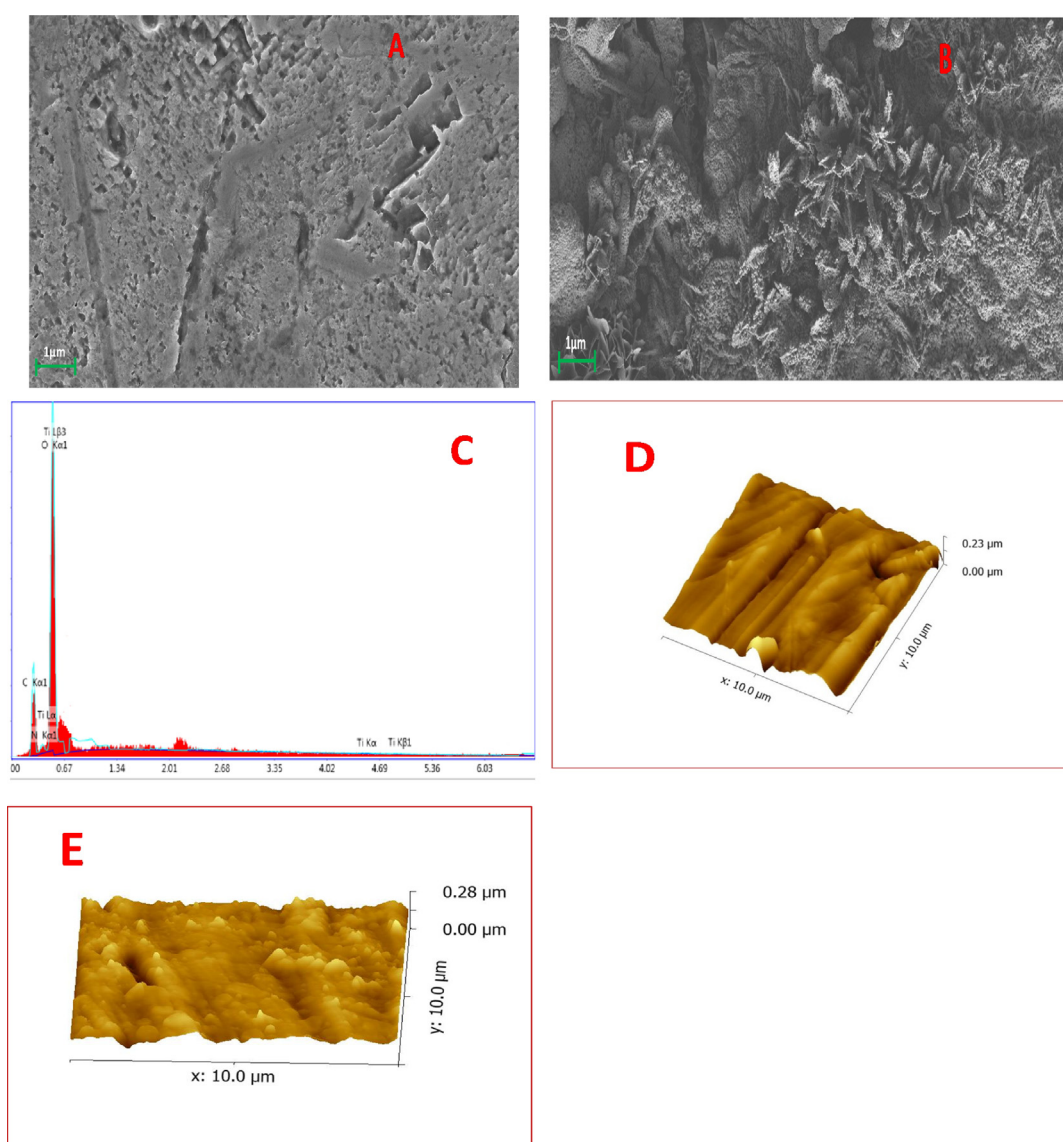


Fig. 3 FESEM image of (A) The damaged mild steel surface (B) TPVA coating (C) corresponding EDAX spectra on mild steel immersed in 3.5 wt% NaCl medium after 40 days. (D) and (E) AFM image showing the surface topography bare mild steel and TPVA coated mild steel respectively.

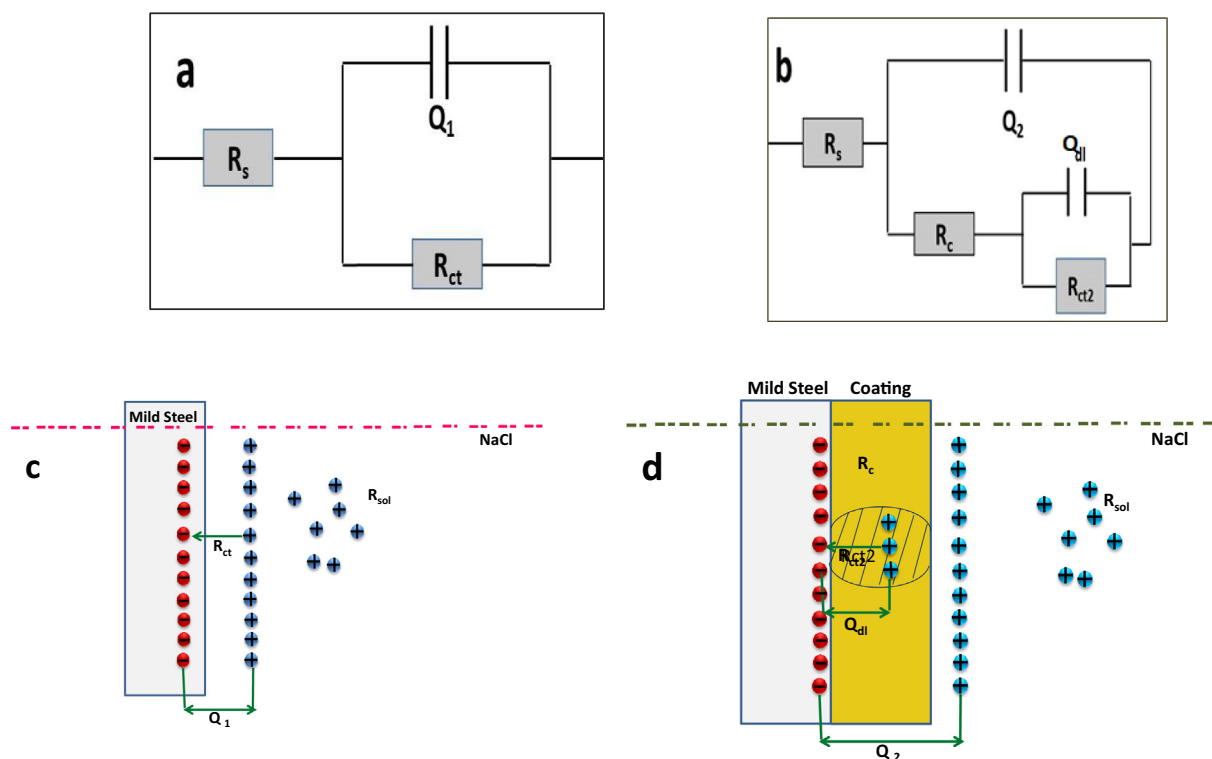


Fig. 4 Proposed Equivalent circuit model and corrosion mechanisms for (a) and (c) bare (b) and (d) modified samples.

3.5. AFM analysis

The topography of coated and bare mild steel generated using 3D AFM technique are given in Fig. 3E and D. The surface roughness (RMS) value obtained for bare and coated mild steel samples are $0.23 \mu\text{m}$, $0.28 \mu\text{m}$ respectively. This value discloses that the addition of PVA into the Titania matrix leads to increase in roughness. The presence of nanoparticles into mild steel matrix is further understood by the hindrance of free movement of the AFM tip (Radwan et al., 2015).

3.6. Monitoring of corrosion inhibition

3.6.1. Impedance spectroscopic studies

EIS is a powerful tool usually employed for the monitoring and prediction of the corrosion and subsidiary processes when coatings are involved (Brassard et al., 2012). The data generated through the EIS studies could be simulated by numerical fitting with Zimp Win software (Gill AC) using the best fit equivalent circuits as shown in Fig. 4A and B. Impedance parameters like solution resistance (R_s), charge transfer resistance (R_{ct}), electric double layer capacitance at the metal/electrolyte interface (Q_{dl}), coating capacitance (Q_2) and double layer capacitance (Q_1) at the metal-coating interface are obtained from impedance studies and data manipulations. In these circuits, CPE_{dl} have been used instead of pure double layer capacitance (C_{dl}) because of the non-ideal character of the impedance responses (Vignesh et al., 2017). The R_{ct} is used to predict the degree of easiness of the corrosion process. As the charge transfer impedance increases the more difficult it

is to react. The R_{ct} was inversely proportional to the defects in the coating on the metal surface. The double layer capacitance, Q_{dl} , was generated by two dissimilar charge layers on the material surface (Cui et al., 2018). Nyquist plots are shown in Fig. 5A and B. The resistance against corrosion in this aggressive medium can be evidenced from the large R_{ct} values. Herein throughout the studies the R_{ct} value of coated sample was higher than bare metal which accounts for the extended barrier property of coating and better resistance towards corrosion in this aggressive saline environment.

It is evident from Fig. 5A and B and table 1 that the coating resistance, as well as charge transfer resistance of coated mild steel, gradually increased with increasing concentration of PVA. A high R_{ct} ($3.2 \times 10^4 \Omega \text{cm}^2$) and low coating capacitance ($112 \mu\text{F}/\text{cm}^2$) value was obtained by TPVA coating in comparison to other coated samples and register an inhibition efficiency of 98.6%. The results further support the view that the increased loading of PVA from 10 to 20 wt% in the TiO_2 matrix led to higher corrosion inhibition performance with impedance modulus of 2.15×10^4 to $3.26 \times 10^4 \Omega \text{cm}^2$. But with 30 wt% PVA ($1.45 \times 10^4 \Omega \text{cm}^2$) the inhibition efficiency showed a reverse tendency and based on these results the order of the corrosion inhibition efficiency is suggested as follows: $\text{TPVA}_1 < \text{TPVA}_2 > \text{TPVA}_3$. It can be concluded well that there is an optimum PVA load is required for improving the corrosion protection properties of the of the material, while higher loading leads to the formation of a breakable film with poor barrier properties may be due to the development of increased defects on the formed sol-gel layer (El-Lateef and Khalaf, 2015). So, here in this study an optimum of 20 wt% of PVA is fixed in TiO_2 which gives higher protection efficiency.

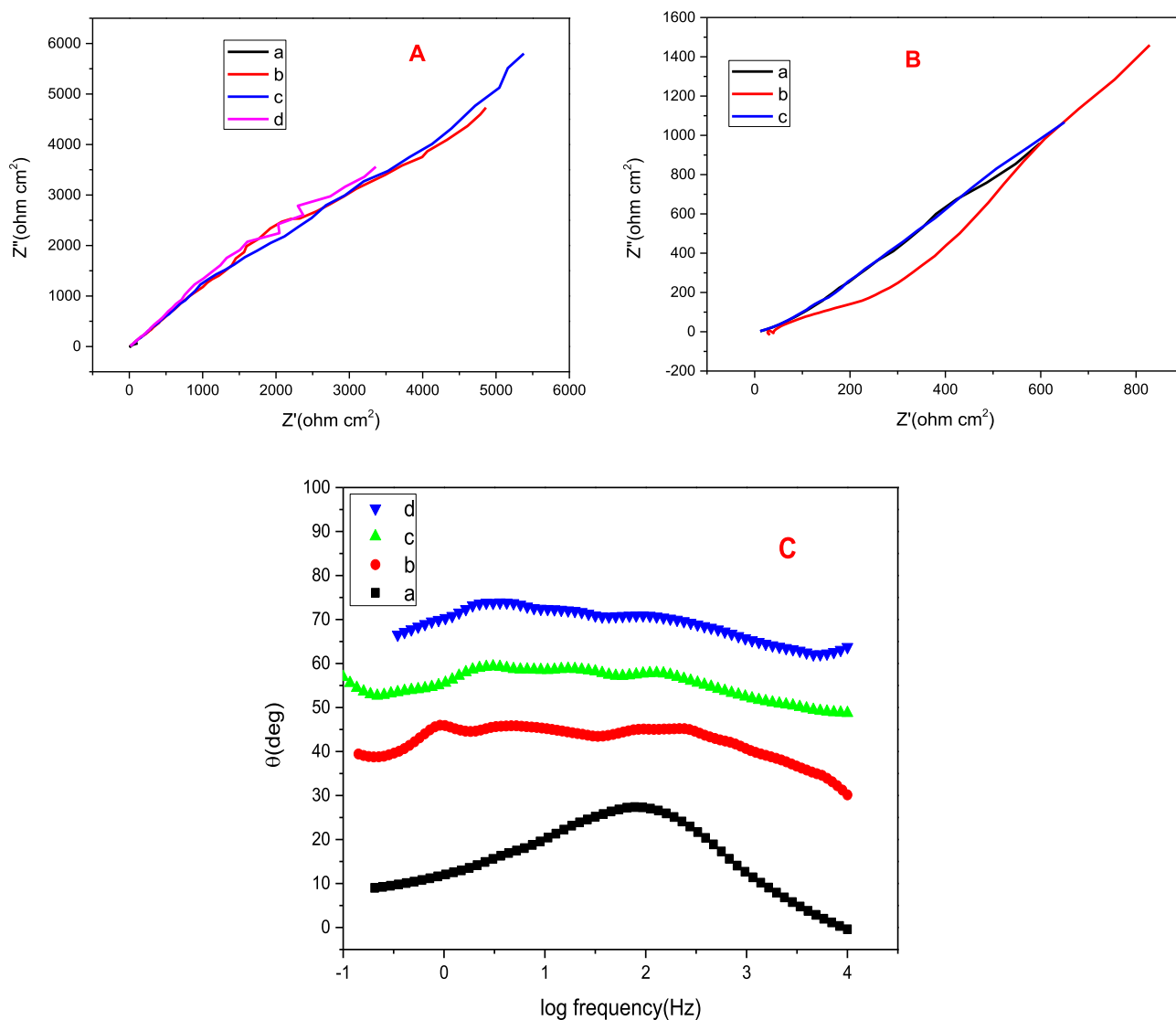


Fig. 5 Nyquist plots for (A) (a) bare mild steel (b) TPVA₁ (c) TPVA (d) TPVA₂ coated on mild steel dried at 200 °C in 3.5 wt% NaCl medium (inset: bare mild steel). (B) TPVA immersed in 3.5 wt% NaCl medium (a) after 15 days (b) 30 days (c) 40 days (C) Frequency vs phase angle plots for (a) (a) bare mild steel (b) TPVA₁ (c) TPVA (d) TPVA₂ coated on mild steel.

Table 1 EIS parameters for bare and MS coated with TiO₂- PVA composite in 3.5 wt% NaCl.

Sample code	$R_s(\Omega \text{ cm}^2)$	$Q (\mu\text{F}/\text{cm}^2)$	$R_c(\Omega\text{cm}^2)$	$Qdl (\mu\text{F}/\text{cm}^2)$	$R_{ct}(\Omega\text{cm}^2)$	I E %
Bare mild steel	1.25	458	–	–	447	
TPVA 1	24.8	198	339.7	3.86	21,548	97.9
TPVA	2.26	112	190.2	2.28	32,600	98.6
TPVA 2	5.46	134	145.2	4.4 4	14,587	96.9
Blank 15 days	3.89	576	–	–	259	
TVA 15 days	33.68	188	616.4	2.8 7	6937	96.3
Blank 30 days	14.65	619	–	–	188	
TVA 30 days	6.96	221	196.3	3.92	3044	93.8
Blank 40 days	8.95	654	–	–	102	
TPVA 40 days	10.94	275	244.9	4.88	1431	92.8

Bode plots of TiO₂- PVA composite are given in Fig. 5C and D, for all coated samples unlike bare mild steel, one-time constant was not observed. Corrosion inhibition efficiency of

TPVA coating on mild steel in 3.5 wt% NaCl for 10, 20, 30 and 40 days were investigated and the obtained impedance parameters were displayed in Fig. 5 and table 1. As evidenced

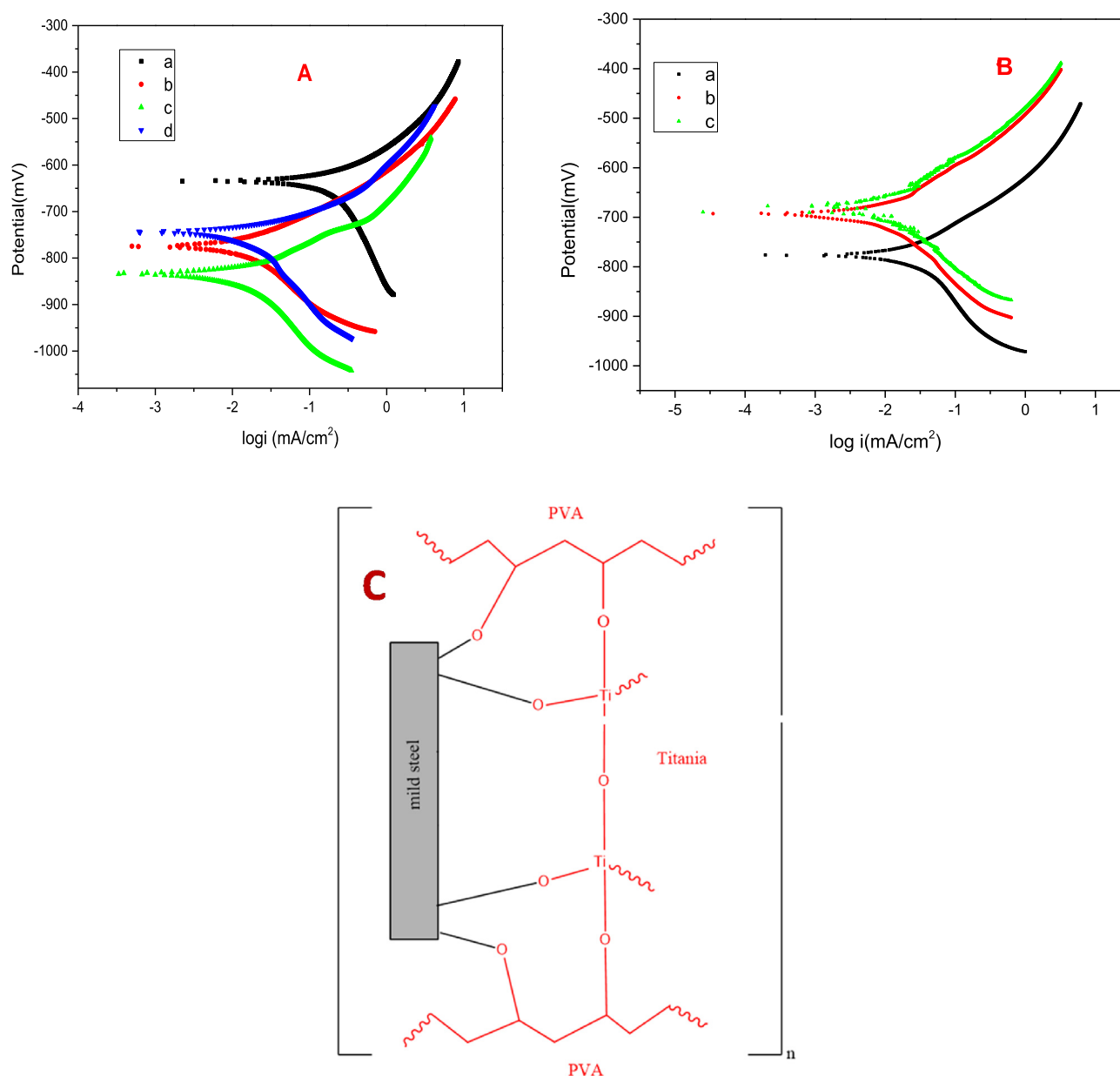


Fig. 6 Tafel plots for (A) (a) bare mild steel (b) TPVA₁ (c) TPVA (d) TPVA₂ coated on mild steel dried at 200 °C in 3.5 wt% NaCl medium. (B) TPVA immersed in 3.5 wt% NaCl medium (a) after 15 days (b) 30 days (c) 40 days (C) Pictorial representation of proposed coating mechanism on mild steel substrate.

from these, during the 1 h – 15 days of immersion, the impedance modulus value was reduced significantly from 3.26×10^4 to $6.97 \times 10^3 \Omega \text{ cm}^2$. During 15–40 days of immersion, very small amount of corrosion products occurred. As the immersion time extended beyond 40 days, the electrolyte penetrated into the coating, and the protection barrier of the coating reduced little and the corresponding impedance modulus value shifted to lower values. Despite this, it has been found that after 40 days of immersion the protection efficiency remained as 92.8% suggesting better performance of the coated specimen and the corresponding morphology (FESEM) and element distribution (EDAX) pattern were given in Fig. 4.

3.6.2. Dynamic polarization studies

Potentiodynamic polarization studies have been widely used to follow the ability of the metallic substrates in aggressive corrosion environments (Balaji and Sethuraman, 2016). Tafel curves of coated and uncoated mild steel recorded after 1 h of immersion in NaCl solution are given in Fig. 6. Both cathodic and anodic Tafel curves show significant shift to lower current densities for these coated samples compared to bare mild steel. Tafel parameters such as corrosion potential (E_{corr}), corrosion current density (I_{corr}), inhibition capacity (IE%), Tafel slopes like β_a and β_c obtained by extrapolation are listed in Table 2. From these results, it can be concluded that I_{corr} decreased with increase in the concentration of PVA which is strong

Table 2 Polarization PDP parameters for bare and MS coated with TiO₂- PVA composite in 3.5 wt% NaCl.

Sample code	$-E_{\text{Corr}}$ (mV)	I_{Corr} (mA/cm ²)	β_a (mV/dec)	β_c (mV/dec)	IE %
Bare mild steel	652	0.2164	119.9	65.3	
TPVA1	727	0.0105	140.8	31.9	95.1
TPVA	774	0.0056	101.6	56.7	97.4
TPVA2	832	0.0081	129.2	41.9	96.2
Blank 15 days	648	0.3054	115.5	79.2	
TVA 15 days	769	0.0096	98.5	85.7	96.8
Blank 30 days	702	0.3998	100.8	95.9	
TVA 30 days	696	0.0234	118.5	78.5	94.1
Blank 40 days	664	0.4959	148	106.2	
TVA 40 days	691	0.03118	108.2	69.7	93.7

evidence for the extended protective nature of the coated steel surface. The I_{corr} of the TPVA was 0.0056 mA/cm² much lower than the corresponding value of bare mild steel (0.2164 mA/cm²). The IE (%) obtained for TPVA₁, TPVA, and TPVA₂ are 95.1, 97.4, and 96.2% respectively. These results are more or less similar to that generated from impedance studies, a totally different approach in which the chance for error is more.

3.6.3. Mechanism of corrosion inhibition

The most probable mechanism is pictorially represented in Fig. 6C. Hydrolysis and condensation reactions of titanium ethoxide results in the formation of Ti-O-Ti sol-gel network. As the surface of TiO₂ possesses large number of -OH groups which enables bond formation with PVA through the condensation type reaction. These weak bonds were transformed into stable covalent bond during the sintering process. TiO₂-PVA hybrid material possess reasonable adhesion to the metal surface via chemical bonding. The Ti-O-Ti, linkage and Fe-Ti-O bond and compactness of the coated surface, could be attributed to the effective blocking of corrosion.

4. Conclusions

- An eco-friendly and economically viable method has been developed for the synthesis of TiO₂ - PVA coating on mild steel, by dip-coating technique and the material was characterized by advanced spectroscopic and microscopic techniques like FTIR, FESEM, EDX, AFM, UV and XRD.
- The corrosion protection behaviour of the hybrid coating on mild steel in NaCl medium was evaluated by using EIS and Tafel methods.
- Effects of PVA loading on corrosion efficiency have also investigated. The results show that an optimum loading of PVA(20 wt%) is required for the corrosion resistance and protection efficiency.
- TPVA coating offers excellent protection to mild steel in 3.5 wt% NaCl for 40 days, which is much greater than the efficiency of conventional coatings in this period of time.
- Without the incorporation of epoxy resins like adhesive materials into the metallic surface TiO₂-TPVA hybrid material can coated with excellent barrier performance.

Acknowledgment

The author Jaseela.P.K.is grateful to Maulana Azad National Fellowship (MANF) for providing financial support and CSIF, university of Calicut for their assistance in characterization techniques.

References

- Anupama, K., Ramya, K., Shainy, K., Joseph, A., 2015. Adsorption and electrochemical studies of Pimenta dioica leaf extracts as corrosion inhibitor for mild steel in hydrochloric acid. *Mater. Chem. Phys.* 167, 28–41.
- Anupama, K., Ramya, K., Joseph, A., 2016. Electrochemical and computational aspects of surface interaction and corrosion inhibition of mild steel in hydrochloric acid by Phyllanthus amarus leaf extract (PAE). *J. Mol. Liq.* 216, 146–155.
- Balaji, J., Sethuraman, M., 2016. Improved corrosion resistance by forming multilayers over a copper surface by electrodeposition followed by a novel sol-gel coating method. *RSC Adv.* 6, 95396–95404.
- Balaji, J., Sethuraman, M., 2017. Chitosan-doped-hybrid/TiO₂ nanocomposite based sol-gel coating for the corrosion resistance of aluminum metal in 3.5% NaCl medium. *Int. J. Biol. Macromol.* 104, 1730–1739.
- Brassard, J.-D., Sarkar, D.K., Perron, J., 2012. Fluorine based superhydrophobic coatings. *Appl. Sci.* 2, 453–464.
- Catauro, M., Bollino, F., Giovanardi, R., Veronesi, P., 2017. Modification of Ti6Al4V implant surfaces by biocompatible TiO₂/PCL hybrid layers prepared via sol-gel dip coating: Structural characterization, mechanical and corrosion behavior. *Mater. Sci. Eng., C* 74, 501–507.
- Chou, T., Chandrasekaran, C., Limmer, S., Seraji, S., Wu, Y., Forbess, M., Nguyen, C., Cao, G., 2001. Organic-inorganic hybrid coatings for corrosion protection. *J. Non-Cryst. Solids* 290, 153–162.
- Cohen, S., 1995. Replacements for chromium pretreatments on aluminum. *Corrosion* 51, 71–78.
- Cui, X., Zhu, G., Pan, Y., Shao, Q., Dong, M., Zhang, Y., Guo, Z., 2018. Polydimethylsiloxane-titania nanocomposite coating: fabrication and corrosion resistance. *Polymer* 138, 203–210.
- Das, K., Panda, S.K., Chaudhuri, S., 2008. Solvent-controlled synthesis of TiO₂ 1D nanostructures: growth mechanism and characterization. *J. Cryst. Growth* 310, 3792–3799.
- Donley, M.S., Mantz, R.A., Khramov, A., Balbyshev, V., Kasten, L. S., Gaspar, D.J., 2003. The self-assembled nanophase particle (SNAP) process: a nanoscience approach to coatings. *Prog. Org. Coat.* 47, 401–415.

- El-Lateef, H.M.A., Khalaf, M.M., 2015. Corrosion resistance of ZrO₂-TiO₂ nanocomposite multilayer thin films coated on carbon steel in hydrochloric acid solution. *Mater. Charact.* 108, 29–41.
- Ge, L., Zhang, M., Wang, R., Li, N., Zhang, L., Liu, S., Jiao, T., 2020. Fabrication of CS/GA/RGO/Pd composite hydrogels for highly efficient catalytic reduction of organic pollutants. *RSC Adv.* 10, 15091–15097.
- Geng, R., Yin, J., Zhou, J., Jiao, T., Feng, Y., Zhang, L., Chen, Y., Bai, Z., Peng, Q., 2020. In Situ Construction of Ag/TiO₂/g-C₃N₄ Heterojunction Nanocomposite Based on Hierarchical Co-Assembly with Sustainable Hydrogen Evolution. *Nanomaterials* 10, 1.
- He, Y., Wang, R., Sun, C., Liu, S., Zhou, J., Zhang, L., Jiao, T., Peng, Q., 2020. Facile Synthesis of Self-Assembled NiFe Layered Double Hydroxide-Based Azobenzene Composite Films with Photoisomerization and Chemical Gas Sensor Performances. *ACS Omega* 5, 3689–3698.
- Jaseela, P., Joseph, A., 2018. Development of Flower Like Hierarchical Thiourea Loaded Titania-Poly Vinyl Alcohol Nano Composite Coatings for the Corrosion Protection of Mild Steel in Hydrochloric Acid. *J. Inorgan. Organometall. Polym. Mater.*, 1–15
- Kang, H., Cheng, Z., Lai, H., Ma, H., Liu, Y., Mai, X., Wang, Y., Shao, Q., Xiang, L., Guo, X., 2018. Superlyophobic anti-corrosive and self-cleaning titania robust mesh membrane with enhanced oil/water separation. *Sep. Purif. Technol.* 201, 193–204.
- Karthik, N., Sethuraman, M.G., 2015. Improved copper corrosion resistance of epoxy-functionalized hybrid sol-gel monolayers by thiosemicarbazide. *Ionics* 21, 1477–1488.
- Kim, T.-H., Rodríguez-González, V., Gyawali, G., Cho, S.-H., Sekino, T., Lee, S.-W., 2013. Synthesis of solar light responsive Fe, N co-doped TiO₂ photocatalyst by sonochemical method. *Catal. Today* 212, 75–80.
- Lakshmi, R., Yoganandan, G., Kavaya, K., Basu, B.J., 2013. Effective corrosion inhibition performance of Ce³⁺ doped sol-gel nanocomposite coating on aluminum alloy. *Prog. Org. Coat.* 76, 367–374.
- Liu, Y., Sun, D., You, H., Chung, J.S., 2005. Corrosion resistance properties of organic-inorganic hybrid coatings on aluminum alloy. *Appl. Surf. Sci.* 246 (2024), 82–89.
- Luo, F., Li, Q., Zhong, X., Gao, H., Dai, Y., Chen, F., 2012. Corrosion electrochemical behaviors of silane coating coated magnesium alloy in NaCl solution containing cerium nitrate. *Mater. Corros.* 63, 148–154.
- Ning, C., Mingyan, L., Weidong, Z., 2012. Fouling and corrosion properties of SiO₂ coatings on copper in geothermal water. *Ind. Eng. Chem. Res.* 51, 6001–6017.
- Palomino, L.E., Aoki, I.V., de Melo, H.G., 2006. Microstructural and electrochemical characterization of Ce conversion layers formed on Al alloy 2024-T3 covered with Cu-rich smut. *Electrochimica Acta* 51, 5943–5953.
- Radwan, A.B., Shakoor, R., Popelka, A., 2015. Improvement in properties of Ni-B coatings by the addition of mixed oxide nanoparticles. *Int. J. Electrochem. Sci* 10, 7548–7562.
- Ramezanzadeh, B., Vakili, H., Amini, R., 2015. The effects of addition of poly (vinyl) alcohol (PVA) as a green corrosion inhibitor to the phosphate conversion coating on the anticorrosion and adhesion properties of the epoxy coating on the steel substrate. *Appl. Surf. Sci.* 327, 174–181.
- Ramya, K., Mohan, R., Anupama, K., Joseph, A., 2015. Electrochemical and theoretical studies on the synergistic interaction and corrosion inhibition of alkyl benzimidazoles and thiosemicarbazide pair on mild steel in hydrochloric acid. *Mater. Chem. Phys.*, 149, pp. 632–647.
- Sinapi, F., Delhalle, J., Mekhalif, Z., 2002. XPS and electrochemical evaluation of two-dimensional organic films obtained by chemical modification of self-assembled monolayers of (3-mercaptopropyl) trimethoxysilane on copper surfaces. *Mater. Sci. Eng., C* 22, 345–353.
- Tsapakos, M.J., Hampton, T., Sinclair, P., Sinclair, J., Bement, W., Wetterhahn, K., 1983. The carcinogen chromate causes DNA damage and inhibits drug-mediated induction of porphyrin accumulation and glucuronidation in chick embryo hepatocytes. *Carcinogenesis* 4, 959–966.
- Van Ooij, W., Child, T., 1998. Protecting metals with silane coupling agents. *Chem. Tech.* 28, 26–35.
- Van Ooij, W., Zhu, D., Prasad, G., Jayaseelan, S., Fu, Y., Teredesai, N., 2000. Silane based chromate replacements for corrosion control, paint adhesion, and rubber bonding. *Surf. Eng.* 16, 386–396.
- Vignesh, R.B., Balaji, J., Sethuraman, M., 2017. Surface modification, characterization and corrosion protection of 1, 3-diphenylthiourea doped sol-gel coating on aluminium. *Prog. Org. Coat.* 111, 112–123.
- Wang, D., Bierwagen, G.P., 2009. Sol-gel coatings on metals for corrosion protection. *Prog. Org. Coat.* 64, 327–338.
- Wang, R., Yan, X., Ge, B., Zhou, J., Wang, M., Zhang, L., Jiao, T., 2020. Facile preparation of self-assembled black phosphorus-dye composite films for chemical gas sensors and surface-enhanced Raman scattering performances. *ACS Sustain. Chem. Eng.* 8, 4521–4536.
- Zhang, H., Banfield, J.F., 2002. Kinetics of crystallization and crystal growth of nanocrystalline anatase in nanometer-sized amorphous titania. *Chem. Mater.* 14, 4145–4154.
- Zhang, D., Liu, J., Jiang, C., Li, P., 2017. High-performance sulfur dioxide sensing properties of layer-by-layer self-assembled titania-modified graphene hybrid nanocomposite. *Sens. Actuators, B* 245, 560–567.
- Zhang, D., Jiang, C., Zhou, X., 2018. Fabrication of Pd-decorated TiO₂/MoS₂ ternary nanocomposite for enhanced benzene gas sensing performance at room temperature. *Talanta* 182, 324–332.
- Zhao, J., Yin, J., Zhong, J., Jiao, T., Bai, Z., Wang, S., Zhang, L., Peng, Q., 2019. Facile preparation of a self-assembled Artemia cyst shell-TiO₂-MoS₂ porous composite structure with highly efficient catalytic reduction of nitro compounds for wastewater treatment. *Nanotechnology* 31, 085603.
- Zheludkevich, M.L., Shchukin, D.G., Yasakau, K.A., Möhwald, H., Ferreira, M.G., 2007. Anticorrosion coatings with self-healing effect based on nanocontainers impregnated with corrosion inhibitor. *Chem. Mater.* 19, 402–411.
- Zhu, D., van Ooij, W.J., 2003. Corrosion protection of AA 2024-T3 by bis-[3-(triethoxysilyl) propyl] tetrasulfide in sodium chloride solution.: Part 2: mechanism for corrosion protection. *Corros. Sci.* 45, 2177–2197.